Note

pubs.acs.org/Biomac

Photoassisted One-Step Aerosol Fabrication of Zwitterionic Chitosan Nanoparticles

Jeong Hoon Byeon,[†] Aditya Kulkarni,[†] Hee-Kwon Kim,[‡] David H. Thompson,[†] and Jeffrey T. Roberts*[,†]

[†]Department of Chemistry, Purdue University, 560 Oval Drive, West Lafayette, Indiana 47907, United States

[‡]Department of Nuclear Medicine, Molecular Imaging & Therapeutic Medicine Research Center, Biomedical Research Institute, Chonbuk National University Medical School and Hospital, Jeonju 561-712, Republic of Korea

ABSTRACT: Zwitterionic chitosan nanoparticles (ZCNPs) were conveniently obtained by a one-step aerosol method, and their potential for the production of biocompatible materials was investigated. A low-molecular-weight chitosan was conjugated with succinic anhydride to produce zwitterionic chitosan (ZC). Collison-atomized ZC droplets were simultaneously UV-irradiated and dried in a tube furnace in a one-step aerosol process to produce particles. The observed cytotoxicities of ZCNPs (85 ± 3.9% cell viability) were similar to unmodified chitosan nanoparticles (CNPs, 88 ± 6.6%) and UV-irradiated ZCNPs (83 ± 3.3%). The aerosol process described in this work allowed facile production and modification of CNPs, which could then be employed for biomedical purposes.

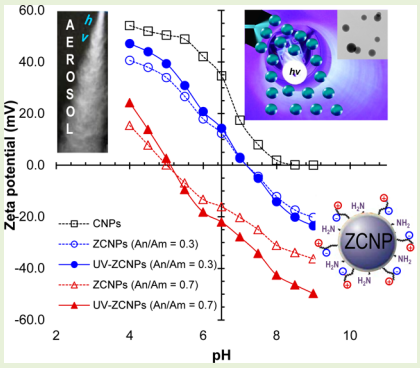

INTRODUCTION

Chitosan, a natural, nontoxic, biocompatible, and biodegradable polymer, is widely used as a gene transfection reagent,[1] in scaffolds for tissue engineering,[2] as a drug delivery substance,[3] and in polymeric coatings for nanoparticles.[4] Because of their cationic properties, however, chitosans are easily cleared by the reticuloendothelial system, severely limiting drug delivery to target tissues.[5] From this point of view, chitosan modification is required to mask the cationic surface and to reduce opsonization[6] for use in a wide range of biomedical applications, including the condensation and intracellular delivery of genetic material.[7−9]

The limited solubility of chitosan at neutral pH provides a unique opportunity to form nanoparticle−drug/gene delivery platforms,[10] but it is also an obstacle if one intends to use chitosan under physiological conditions.[11] Zwitterionic chitosan (ZC), created by the amidation of primary amines of chitosan with succinic anhydride, has recently been reported as a modified form of chitosan that is soluble at neutral pH and can be used as a macromolecular drug carrier.[12−14] Modified chitosan shows a unique pH-dependent charge profile, which, in principle, could be conveniently exploited to create a pH-sensitive coating on the cationic carrier surface.[12]

Many formulations of chitosan-based systems exist as colloidal liquids, usually synthesized using time-consuming batch wet chemical processes and which are generally stable only for short periods of time. Also, some polymer-based systems are specifically designed to be gradually degradable by hydrolysis, making long-term storage in liquid form not a viable option.[15,16] In addition, many formulations are unstable as liquid suspensions for a variety of reasons, including degradation of the carrier and/or active substance, formation of insoluble aggregates, and unwanted loss of bioactivity.[17,18] One approach for overcoming such stability limitations is to formulate and store dry powders. In contrast with classical wet chemical methods, aerosol processing involves a much more limited number of preparation steps. It also produces material continuously, allowing for a straightforward collection of powders and generating low waste.[19] Dry particles can be formulated in the aerosol state by atomizing liquid solutions in an appropriate carrier gas and removing solvent from the resulting particles.[20] Processing is highly reproducible, relatively easy to scale up, and offers uniform particle-size distributions.[21]

The purpose of the present work is to fabricate ZC nanoparticles (ZCNPs) using a one-step aerosol method and to explore the effects of UV irradiation on its surface charge and in vitro cytotoxicity. Chitosan was first modified into ZC and then aerosol-processed and collected to assess in vitro cytotoxicity in HeLa cells using chitosan as a benchmark. Photolytic reactions caused by UV irradiation may induce an increase in surface polarity on the ZCNPs. The rise in the surface polarity of particles is probably due to the photodegradation of glycosidic bonds and pyranose rings.[22] Free radicals formed during UV irradiation may react with atmospheric oxygen, leading to the formation of different types of carbonyl and hydroxyl groups altering the surface property of the ZCNPs.

METHODS

Aerosol Fabrication of ZC. ZCNPs were synthesized by the modification of a method reported by Xu et al.[12] Chitosan (1 g, M_w: 15 000 Da, Polysciences, U.S.) was dissolved in 800 mL of 1 v/v % acetic

Received: April 11, 2014
Revised: May 6, 2014
Published: May 15, 2014

   dx.doi.org/10.1021/bm5005417 | *Biomacromolecules* 2014, 15, 2320−2325

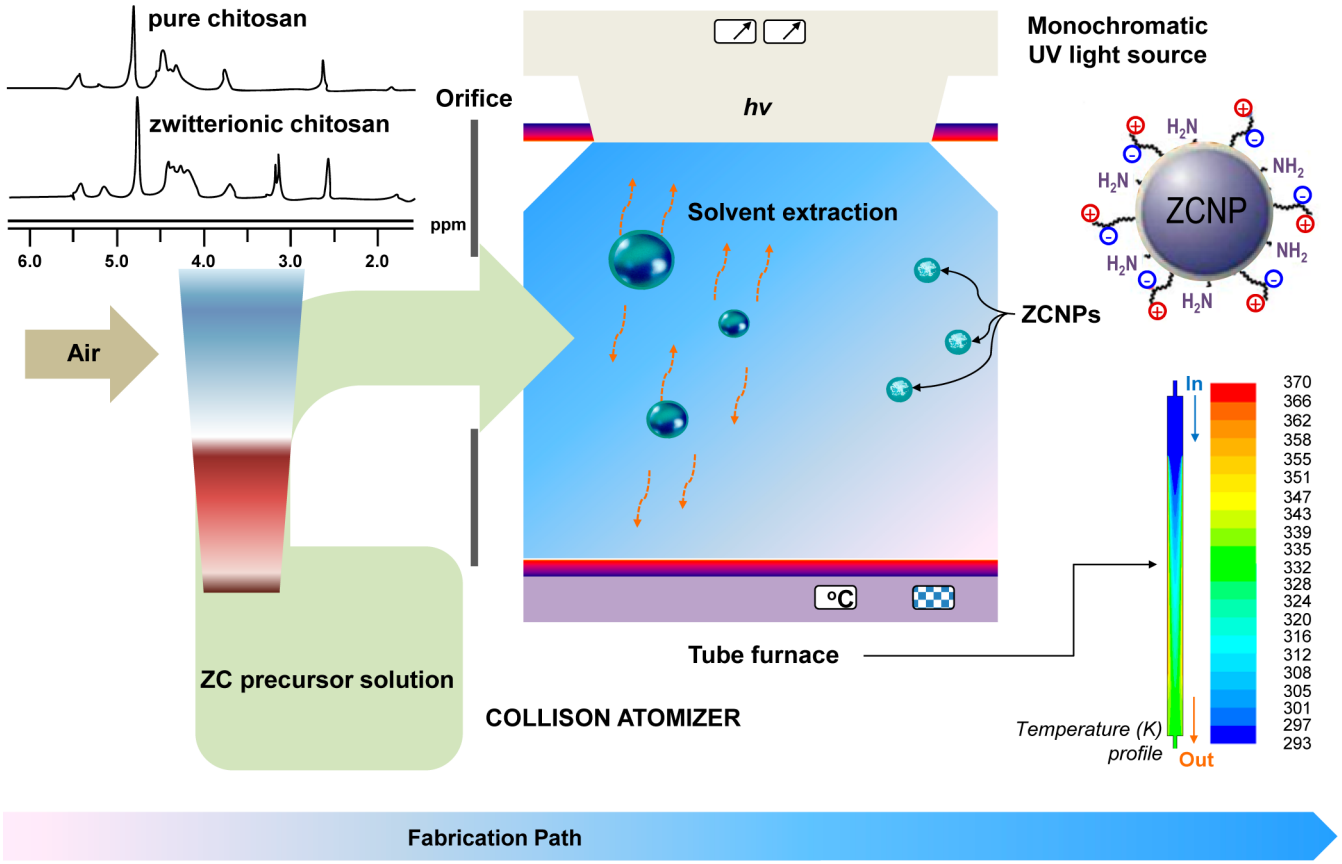

Figure 1. Schematic illustration of photoassisted fabrication of ZCNPs using a one-step aerosol system of a collison atomizer, a UV irradiator, and a heated tube reactor. NMR spectra of pure chitosan nanoparticles and ZCNPs are also shown as insets.

acid solution. The chitosan solution was stirred for 30 min at room temperature. A solution of succinic anhydride in acetone was added to the chitosan solution in the desired molar ratio of succinic anhydride to chitosan amine (An/Am ratio) and was stirred for 30 min at room temperature. For example, for an An/Am ratio of 0.3, 150 mg of succinic anhydride was added to 1 g of chitosan. After stirring for 30 min, 0.1 M NaOH was added to the mixture until the pH of the reaction mixture reached 8. The mixture was then stirred for 15 h at room temperature. The reaction mixture was dialyzed against water (molecular weight cutoff: 3500), whose pH was adjusted to 10 to 11 with 1.0 M NaOH.

Schematic diagrams of the one-step aerosol fabrication used for these experiments are shown in Figure 1. A particle free air flow, which was controlled by a mass flow controller (3810DS, Kofloc, Japan), had a flow rate of 3 L min^{-1}, and was used as the operating gas for atomizing the prepared ZC solution. The droplets were then exposed to 254 nm radiation (LOT-ORIEL, Germany) in a heated tube reactor (760 μW cm^{-2} intensity and 90 °C wall temperature, 1.7 min residence time) to apply phototreatment and simultaneous solvent extraction of the droplets. Figure 1 also shows the ^{1}H NMR (Inova 300, Varian, U.S.) spectra of the ZCNPs and chitosan nanoparticles (CNPs). The CNPs showed signals at chemical shifts of 2.5 to 2.7 ppm (assigned to $-NHCOC\mathbf{H}_2C\mathbf{H}_2COOH$), 3.5 to 4.5 ppm [H2 of *N*-acetyl glucosamine (GlcNAc), H3−H6 of GlcNAc, and glucosamine (GlcN)], and 4.8 ppm (H1 of GlcN). The ZCNPs (An/Am = 0.5) showed additional signals at chemical shifts of 3.15 ppm (H2 of GlcN) and 4.3 ppm ($-N\mathbf{H}COCH_2CH_2COOH$).[23]

Instrumentation. Size distributions of aerosol particles were measured using a scanning mobility particle sizer (SMPS), consisting of a differential mobility analyzer (3081, TSI, U.S.), electrostatic classifier (3080, TSI, U.S.), condensation particle counter (3776, TSI, U.S.), and soft X-ray charger (4530, HCT, Korea). The SMPS system, which was used to measure the mobility equivalent diameter, was operated at a sample flow of 0.3 L min^{-1}, a sheath flow of 3.0 L min^{-1}, and a scan time of 135 s (measurement range: 15.1−661.2 nm). The mass (m) of the CNPs and ZCNPs was measured using a microbalance (DV215CD, Ohaus, Switzerland) and also confirmed via the following equation

$$m = Q \cdot t_s \int_0^\infty \eta(D_p) C_m(D_p)\, dD_p \quad (1)$$

where Q is the flow rate of nitrogen gas, t_s is the sampling time, $\eta(D_p)$ is the fractional collection efficiency, and $C_m(D_p)$ is the mass concentration of particles.

Transmission electron microscope images (CM-100, FEI/Philips, U.S.) were obtained at an accelerating voltage range of 46−180 kV. Specimens were prepared for examination by direct electrostatic aerosol sampling at a sampling flow of 0.5 L min^{-1} and an operating voltage of 5 kV using a nanoparticle collector (NPC-10, HCT, Korea).

For Fourier transform infrared (FTIR) spectroscopy analysis, samples were prepared using polytetrafluoroethylene media substrate (0.2 μm pore size, 47 mm diameter, 11807-47-N, Sartorius, Germany) by physical filtration (i.e., mechanical filtration mainly by diffusion, of particles on the surfaces of the substrate), and the spectra were recorded on a Nicolet 6700 FTIR spectrometer (Thermo Electron, U.S.). The spectra were taken for samples in the range of 4000−400 cm^{-1} in absorbance mode.

The zeta potentials of ZCNPs/plasmid DNA (pDNA) complexes were determined using a zeta potential analyzer (Nano ZS-90, Malvern Instruments, U.K.). The ZCNPs were mixed with pDNA and incubated at room temperature for 30 min. The complexes were then diluted with doubly deionized water to an appropriate concentration. Measurements of the zeta potential were carried out at 25 °C and calculated using the manufacturer's supplied software. The measurements were performed in triplicate, and the results were reported as means.

In Vitro Cytotoxicity. The cytotoxicity of the ZCNPs was evaluated using HeLa cells via the MTS [3-(4,5-dimethyl-thiazol-2-yl)-5-(3-

dx.doi.org/10.1021/bm5005417 | *Biomacromolecules* 2014, 15, 2320−2325

carboxymethoxyphenyl)-2-(4-sulfophenyl)-2*H*-tetrazolium] assay. Cells were cultured in 200 mL of Dulbecco's modified Eagle medium (DMEM, Carlsbad, U.S.) supplemented with 10% fetal bovine serum (FBS) at 37 °C, 5% CO_2, at 95% relative humidity. The cells were seeded in a 96-well microtiter plate (Nunc, Germany) at densities of 1×10^5 cells well^{-1}. After 24 h, the culture media was replaced with serum-supplemented culture media containing the ZCNPs (1 mg mL^{-1}), and the cells were incubated for 24 h. MTS reagent (30 μL) was then added to each well. Cells were incubated for an additional 2 h. Absorbances were measured using a microplate reader (Spectra Plus, TECAN, Switzerland) at a wavelength of 490 nm. The cell viability (%) was compared with that of the untreated control cell in media without ZCNPs and calculated using $[A]_{test}$:$[A]_{control} \times 100\%$, where $[A]_{test}$ is the absorbance of the wells with ZCNPs and $[A]_{control}$ is the absorbance of the control wells. All experiments were performed in triplicate, and the results were reported as means and standard deviations. Statistical analyses were performed using Student's *t* test. The differences were considered significant for $p < 0.05$.

RESULTS AND DISCUSSION

Figure 2 summarizes the size distribution measurements of ZCNPs. The geometric mean diameter (GMD), geometric

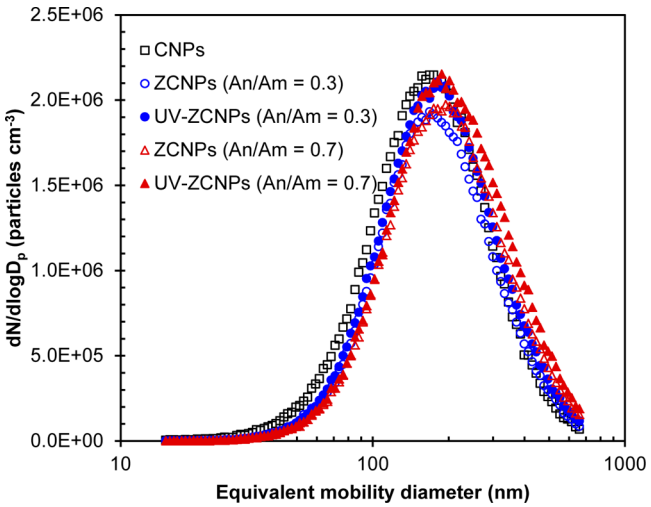

Figure 2. Aerosol size distributions of CNPs and ZCNPs.

standard deviation (GSD), and total number concentration (TNC) of the CNPs were 164.6 nm, 1.71, and 1.23×10^6 cm^{-3}, respectively. Analogous data for ZCNPs (An/Am = 0.3) and ZCNPs (An/Am = 0.7) with and without UV irradiation were noted in Table 1. The size distribution of the ZCNPs (An/Am = 0.7) was slightly larger than that for ZCNPs (An/Am = 0.3). This implies that a higher An/Am ratio may induce an increase in the aerosol size, and the UV irradiation did slightly increase the size distribution.

Table 1. Aerosol Size Distributions of CNPs and ZCNPs

case	GMD (nm)	GSD (−)	TNC (particles cm^{-3})
CNPs	164.6	1.71	1.23×10^6
ZCNPs (An/Am = 0.3)	176.5	1.67	1.06×10^6
UV-ZCNPs (An/Am = 0.3)	180.4	1.68	1.16×10^6
ZCNPs (An/Am = 0.7)	189.7	1.69	1.12×10^6
UV-ZCNPs (An/Am = 0.7)	195.2	1.69	1.22×10^6

TEM images (Figure 3) indicate that all ZCNPs have roughly spherical shapes, with smooth surfaces. Particles are also well-separated. The particles exhibit boundaries between a core (dark, dense solid) section and a shell (bright, light solid) section. The formation of spherical particles is attributed to the slow convective drying rate, for which the time for liquid evaporation was greater than the time required for supersaturated particles at a liquid−vapor interface to migrate back toward the droplet center. The Peclet number, *Pe*, is a dimensionless number that expresses the relative time-scales for diffusion ($D_d^2/4\delta_v$) and convective drying (τ_d).

$$Pe = \frac{D_d^2}{4\tau_d \delta_v} \tag{2}$$

For the present case, conditions were such that $Pe \ll 1$, ensuring that migration of solutes from the interface toward the droplet center was sufficient to keep up with convective drying. When An/Am ratio increased from 0.3 to 0.7, there was no observable change in particle morphology. Similarly, UV-irradiated particles showed similar morphology. This indicates that the ZCNPs were not significantly dissociated or oxidized during UV irradiation. The mean-mode diameters of the ZCNPs (0.3 An/Am) and their UV-treated cases were 178 ± 8.9 and 181 ± 9.3 nm, respectively. The same data for ZCNPs (0.7 An/Am) were 188 ± 10.0 and 193 ± 11.3 nm, respectively, and these data are consistent with the data described in Figure 2 and Table 1

To clarify the structural modifications of the CNPs from succinic anhydride- and UV-treated nanoparticles, we obtained FTIR spectra of CNPs and ZCNPs particles (Figure 4). For CNPs, the IR spectrum exhibits the typical absorption bands at 3359, 2920, and 2880 cm^{-1}, which attributed, respectively, to the stretching vibrations of −OH, $-CH_2$, and $-CH_3$ groups.[24] Characteristic bands at 1683, 1566, and 1382 cm^{-1} can be assigned to amide I (C═O stretch), amide II (C−N stretch, C−N−H bend), and amide III (C−N stretch, C−N−H bend), respectively. The band peaks at 1409 and 1316 cm^{-1} correspond to the vibrations of the −OH and −CH groups in the pyranose ring. For ZCNPs, a prominent band at 1565 cm^{-1} was assigned to the bending vibration of N−H amides (amide II) due to the existence of succinyl groups (*N*-succinylation).[25] This bending vibration in the case at An/Am = 0.7 was more distinct than that of An/Am = 0.3. Moreover, in the case at An/Am = 0.7, a band at 1720 cm^{-1} was ascribed to the −C═O carbonyl stretching vibration of amides (amide I) and *O*-succinylation in addition to *N*-succinylation, explaining the high degree of succinylation of chitosan. Also, the appearance of the peak at 2370 cm^{-1} corresponding to the −CN group confirmed the incorporation of the succinyl groups on the chitosan backbone. Table 2 summarizes the position of bands in IR spectra of ZCNPs before and after UV irradiation. The A_{-OH}/A_{amide} ratio for ZCNPs calculated from the IR data was smaller than that for CNPs due to a partial conjugation of the amine groups of chitosan with succinyl groups. The results also show that the position of the bands did not change significantly with UV irradiation. The A_{-OH}/A_{amide} ratio for ZCNPs decreased after UV irradiation, especially in the case at An/Am = 0.7. We attribute these changes to photodegradation process of the pyranose rings, resulting in the formation of the carbonyl and amide groups.[26] The C−N bond strength in the amide group is low (~53 kcal mol^{-1}) and can be readily photolyzed, and the resulting radical may abstract hydrogen to form an amine. This mechanism was observed in the case of both aliphatic and aromatic polyamides at the 254 nm irradiation.[22]

dx.doi.org/10.1021/bm5005417 | *Biomacromolecules* 2014, 15, 2320−2325

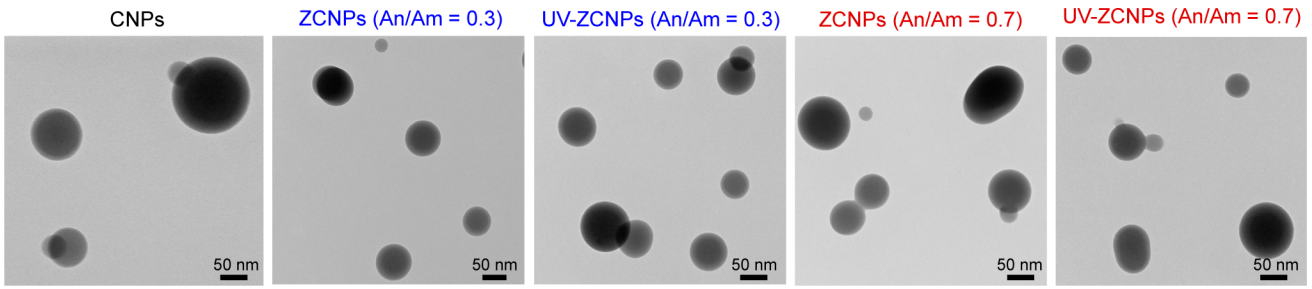

Figure 3. TEM images of CNPs and ZCNPs.

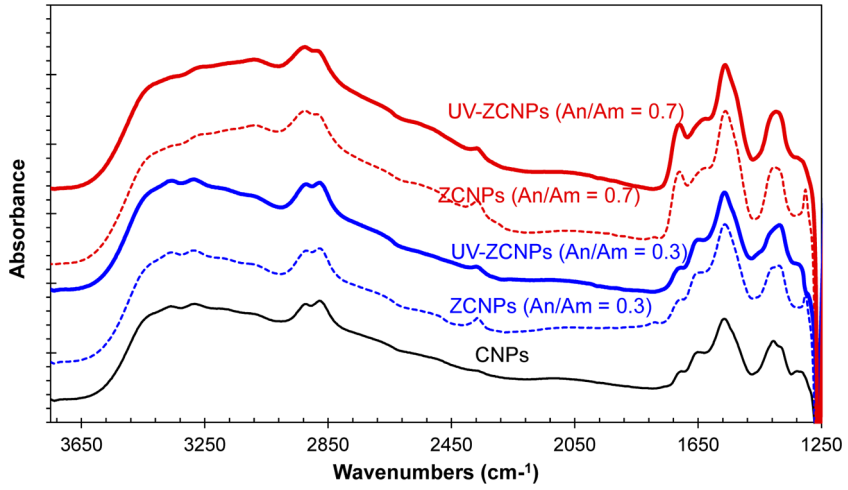

Figure 4. FTIR spectra of CNPs and ZCNPs samples.

Table 2. Position of Bands in FTIR Spectra of CNPs and ZCNPs Samples

	groups				
samples	−OH	−NH stretching	C═O amide I bond	−NH bending in amide group	A_{-OH}/A_{amide}
	bands position (cm^{-1})				
CNPs	3359	3282	1683	1566	1.33
ZCNPs (An/Am = 0.3)	3355	3286	1687	1564	1.13
UV-ZCNPs (An/Am = 0.3)	3356	3284	1677	1564	1.05
ZCNPs (An/Am = 0.7)	3351	3255	1708	1587	1.04
UV-ZCNPs (An/Am = 0.7)	3336	3251	1710	1562	0.88

The zeta potential of the CNPs and ZCNPs was measured at different pH values. The ZCNPs were positive at acidic pH and negative at basic pH (Figure 5). The isoelectric point of ZCNPs decreased from 7.2 to 5.0 with an increase in the An/Am ratio from 0.3 to 0.7. The polarity did not change markedly, but the polarity of the surface increased with UV irradiation. The increase in the polarity of the samples indicated efficient photooxidation on the surface, with the formation of new polar groups on the polymer backbone. ZC macroradicals formed during UV irradiation may interact with each other; then, these radicals can undergo recombination. In particular, the active OH radicals derived from irradiated ZCNPs can interact with succinyl macromolecules and produce new radicals and macroradicals. In ZCNPs, macromolecules there are many OH groups on the chitosan molecule; therefore, many active OH radicals and macroradicals can be formed. The zeta potentials of CNPs/pDNA and ZCNPs/pDNA complexes are described in Table 3 The data show that the net negative charge of the complexes varied with different surface properties. The increased negative potentials are attributed to binding between ZCNPs and negatively charged pDNA.

The cytotoxicity of the ZCNPs/pDNA complexes at different concentrations, such as 1, 5, 10, 20, and 50 $\mu g\ mL^{-1}$, was evaluated by MTS assay in HeLa cells, in comparison with CNPs/pDNA (Figure 6). Results show that the range of average cell viability with the different mass concentrations was 78−90% for all of the tested ZCNPs. It was observed that the ZCNPs exhibited a higher toxicity at a high particle concentration. Nevertheless, the range of cell viability was similar to that observed for CNPs (83−93%). This implies that the aerosol-fabricated ZCNPs warrant further investigation. The slightly higher cytotoxicity of the ZCNPs was considered to be a consequence of damage from interactions with plasma membranes or other cellular compartments.[27] Therefore, the fact that the cell viability of all ZCNPs was slightly lower suggested that the modification of chitosan was acceptable in vitro. On the basis of this, we are currently modifying this method that is appropriate (comparable to lipofectamine, one of

dx.doi.org/10.1021/bm5005417 | *Biomacromolecules* 2014, 15, 2320−2325

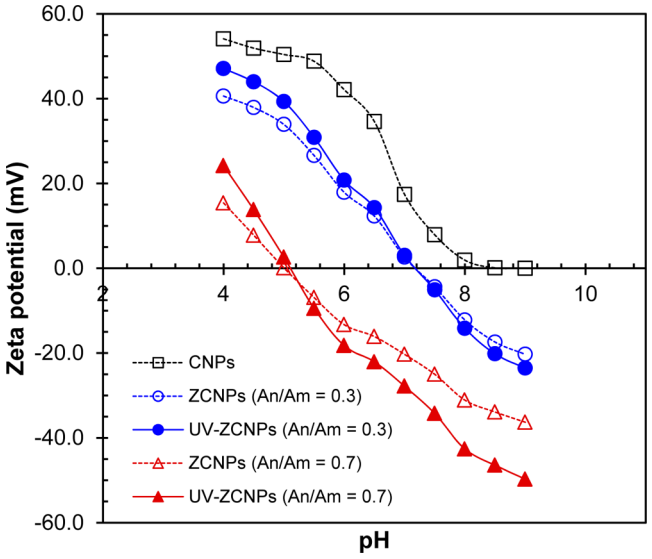

Figure 5. Zeta potential of CNPs and ZCNPs samples.

Table 3. Zeta Potential of pDNA Complexes with ZCNPs Samples

samples/pDNA polyplexes	zeta potential (mV)
CNPs	−1.64 ± 0.66
ZCNPs (An/Am = 0.3)	−14.1 ± 2.11
UV-ZCNPs (An/Am = 0.3)	−15.6 ± 2.85
ZCNPs (An/Am = 0.7)	−32.8 ± 4.41
UV-ZCNPs (An/Am = 0.7)	−39.1 ± 5.58

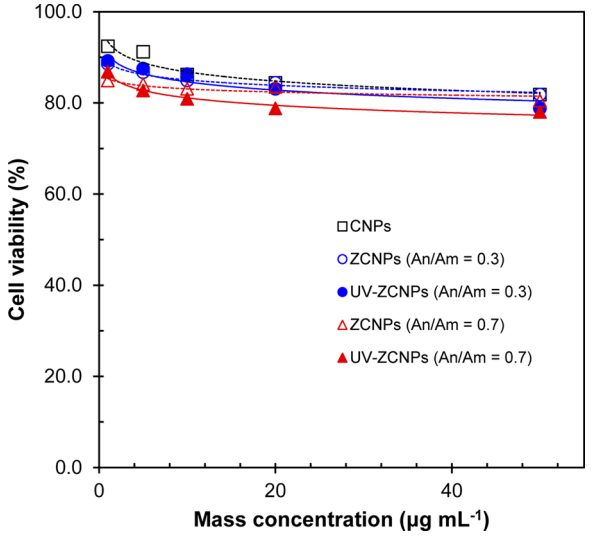

Figure 6. Cytotoxicity of ZCNPs in HeLa cells in comparison with CNPs.

commercial transfection reagents) for gene delivery into HeLa cells at the in vitro level.

CONCLUSIONS

The photoassisted one-step aerosol fabrication of ZCNPs has been performed, and their cytotoxicity was evaluated in vitro. It was shown that the zwitterionic modification of chitosan could achieve a change in the surface charge properties and that this could be further modified by UV irradiation during aerosol fabrication. Compared with CNPs, the cell viability upon exposure to ZCNPs suggested that they have low toxicity, even in the UV irradiation cases. These results will provide some useful evidence of fabrication, which is efficient, green, scalable, and generalizable to biomedical purposes, such as antimicrobial agents, stabilizing agents, and drug carriers.

AUTHOR INFORMATION

Corresponding Author

*E-mail: jtrob@purdue.edu. Tel: (+1-765) 494-1730. Fax: (+1-765) 494-1736.

Notes

The authors declare no competing financial interest.

ACKNOWLEDGMENTS

This work was partially supported by NSF grant CHE-0924431.

REFERENCES

(1) Duceppe, N.; Tabrizian, M. Advances in using chitosan-based nanoparticles for in vitro and in vivo drug and gene delivery. *Expert Opin. Drug Delivery* **2010**, *7*, 1191−1207.

(2) Madihally, S. V.; Matthew, H. W. T. Porous chitosan scaffolds for tissue engineering. *Biomaterials* **1999**, *20*, 1133−1142.

(3) Liang, X. F.; Wang, H. J.; Luo, H.; Tian, H.; Zhang, B. B.; Hao, L. J.; Teng, J. I.; Chang, J. Characterization of novel multifunctional cationic polymeric liposomes formed from octadecyl quaternized carboxymethyl chitosan/cholesterol and drug encapsulation. *Langmuir* **2008**, *24*, 7147−7153.

(4) Nandanan, E.; Jana, N. R.; Ying, J. Y. Functionalization of gold nanospheres and nanorods by chitosan oligosaccharide derivatives. *Adv. Mater.* **2008**, *20*, 2068−2073.

(5) Satija, J.; Gupta, U.; Jain, N. K. Pharmaceutical and biomedical potential of surface engineered dendrimers. *Crit. Rev. Ther. Drug Carrier Syst.* **2007**, *24*, 257−306.

(6) Owens, D. E.; Peppas, N. A. Opsonization, biodistribution, and pharmacokinetics of polymeric nanoparticles. *Int. J. Pharm.* **2006**, *307*, 93−102.

(7) Saranya, N.; Moorthi, A.; Saravanan, S.; Devi, M. P.; Selvamurugan, N. Chitosan and its derivatives for gene delivery. *Int. J. Biol. Macromol.* **2011**, *48*, 234−238.

(8) Kim, T.-H.; Jiang, H.-L.; Jere, D.; Park, I.-K.; Cho, M.-H.; Nah, J.-W.; Choi, Y.-J.; Akaike, T.; Cho, C.-S. Chemical modification of chitosan as a gene carrier in vitro and in vivo. *Prog. Polym. Sci.* **2007**, *32*, 726−753.

(9) Thanou, M.; Nihot, M. T.; Jansen, M.; Verhoef, J. C.; Junginger, H. E. Mono-n-carboxymethyl chitosan (MCC), a polyampholytic chitosan derivative, enhances the intestinal absorption of low molecular weight heparin across intestinal epithelia in vitro and in vivo. *J. Pharm. Sci.* **2001**, *90*, 38−46.

(10) Bowman, K.; Leong, K. W. Chitosan nanoparticles for oral drug and gene delivery. *Int. J. Nanomed.* **2006**, *1*, 117−128.

(11) van der Merwe, S. M.; Verhoef, J. G.; Verheijden, J. H. M.; Kotzé, A. F.; Junginger, H. E. A. Trimethylated chitosan as polymeric absorption enhancer for improved peroral delivery of peptide drugs. *Eur. J. Pharm. Biopharm.* **2004**, *58*, 225−235.

(12) Xu, P.; Bajaj, G.; Shugg, T.; Van Alstine, W. G.; Yeo, Y. Zwitterionic chitosan derivatives for pH-sensitive stealth coating. *Biomacromolecules* **2010**, *11*, 2352−2358.

(13) Kato, Y.; Ohishi, H.; Machida, Y. Biological fate of highly-succinylated N-succinyl-chitosan and antitumor characteristics of its water-soluble conjugate with mitomycin C at i.v. and i.p. administration into tumor-bearing mice. *Biol. Pharm. Bull.* **2000**, *23*, 1497−1503.

(14) Le-Tien, C.; Millette, M.; Mateescu, M.-A.; Lacroix, M. Modified alginate and chitosan for lactic acid bacteria immobilization. *Biotechnol. Appl. Biochem.* **2004**, *39*, 347−354.

(15) Craig, D. Q. M. The mechanisms of drug release from solid dispersions in water-soluble polymers. *Int. J. Pharm.* **2002**, *231*, 131−144.

(16) Bulmus, V.; Chan, Y.; Nguyen, Q.; Tran, H. L. Synthesis and characterization of degradable p(HEMA) microgels: use of acid-labile crosslinkers. *Macromol. Biosci.* **2007**, *7*, 446−455.
(17) Flores-Fernández, G. M.; Solá, R. J.; Griebenow, K. The relation between moisture-induced aggregation and structural changes in lyophilized insulin. *J. Pharm. Pharmacol.* **2009**, *61*, 1555−1561.
(18) Thompson, C. J.; Hansford, D.; Higgins, S.; Rostron, C.; Hutcheon, G. A.; Munday, D. A. Preparation and evaluation of microspheres prepared from novel polyester-ibuprofen conjugates blended with non-conjugated ibuprofen. *J. Microencapsul.* **2009**, *26*, 676−683.
(19) Boissiere, C.; Grosso, D.; Chaumonnot, A.; Nicole, L.; Sanchez, C. Aerosol route to functional nanostructured inorganic and hybrid porous materials. *Adv. Mater.* **2011**, *23*, 599−623.
(20) Ré, M.-I. Formulating drug delivery systems by spray drying. *Drying Technol.* **2006**, *24*, 433−446.
(21) Rizi, K.; Green, R. J.; Donaldson, M.; Williams, A. C. Production of pH-responsive microparticles by spray drying: investigation of experimental parameter effects on morphological and release properties. *J. Pharm. Sci.* **2011**, *100*, 566−579.
(22) Andrady, A. L.; Torikai, A.; Kobatake, T. Spectral sensitivity of chitosan photodegradation. *J. Appl. Polym. Sci.* **1996**, *62*, 1465−1471.
(23) Vanichvattanadecha, C.; Supaphol, P.; Nagasawa, N.; Tamada, M.; Tokura, S.; Furuike, T.; Tamura, H.; Rujiravanit, R. Effect of gamma radiation on dilute aqueous solutions and thin films of N-succinyl chitosan. *Polym. Degrad. Stab.* **2010**, *95*, 234−244.
(24) Praxedes, A. P. P.; da Silva, R. C.; Lima, R. P. A.; Tonholo, J.; Ribeiro, A. S.; de Oliveira, I. N. Effects of UV irradiation on the wettability of chitosan films containing dansyl derivatives. *J. Colloid Interface Sci.* **2012**, *376*, 255−261.
(25) Monier, M.; Wei, Y.; Sarhan, A. A.; Ayad, D. M. Synthesis and characterization of photo-crosslinkable hydrogel membranes based on modified chitosan. *Polymer* **2010**, *51*, 1002−1009.
(26) Sionkowska, A.; Skopinska-Wisniewska, J.; Planecka, A.; Kozlowska, J. The influence of UV irradiation on the properties of chitosan films containing keratin. *Polym. Degrad. Stab.* **2010**, *95*, 2486−2491.
(27) Ma, K.; Hu, M.-X.; Qi, Y.; Zou, J.-H.; Qiu, L.-Y.; Jin, Y.; Ying, X.-Y.; Sun, H.-Y. PAMAM-triamcinolone acetonide conjugate as a nucleus-targeting gene carrier for enhanced transfer activity. *Biomaterials* **2009**, *30*, 6109−6118.